The Importance of Strong Carbon–Metal Adhesion for Catalytic Nucleation of Single-Walled Carbon Nanotubes

ARTICLE *in* NANO LETTERS · MARCH 2008

Impact Factor: 13.59 · DOI: 10.1021/nl072431m · Source: PubMed

7 AUTHORS, INCLUDING:

Feng Ding
The Hong Kong Polytechnic University
117 PUBLICATIONS **3,014** CITATIONS
SEE PROFILE

Andreas Larsson
Luleå University of Technology
56 PUBLICATIONS **998** CITATIONS
SEE PROFILE

Arne Rosén
University of Gothenburg
304 PUBLICATIONS **5,517** CITATIONS
SEE PROFILE

Kim Bolton
Högskolan i Borås
140 PUBLICATIONS **2,548** CITATIONS
SEE PROFILE

NANO LETTERS

xxxx
Vol. 0, No. 0
A−F

The Importance of Strong Carbon–Metal Adhesion for Catalytic Nucleation of Single-Walled Carbon Nanotubes

Feng Ding,[†,⊥,#] Peter Larsson,[‡,#] J. Andreas Larsson,[§,#] Rajeev Ahuja,[‡] Haiming Duan,[†] Arne Rosén,[*,†] and Kim Bolton[†,||]

Physics Department, Göteborg University, SE-412 96, Göteborg, Sweden, Condensed Matter Theory Group, Department of Physics, Uppsala University, Box 530, SE-751 21 Uppsala, Sweden, Tyndall National Institute, University College Cork, Lee Maltings, Prospect Row, Cork, Ireland, School of Engineering, University College of Borås, SE-501 90, Borås, Sweden, and ME & MS Department, Rice University, Houston, Texas 77005

Received September 21, 2007; Revised Manuscript Received December 11, 2007

ABSTRACT

Density functional theory is used to show that the adhesion between single-walled carbon nanotubes (SWNTs) and the catalyst particles from which they grow needs to be strong to support nanotube growth. It is found that Fe, Co, and Ni, commonly used to catalyze SWNT growth, have larger adhesion strengths to SWNTs than Cu, Pd, and Au and are therefore likely to be more efficient for supporting growth. The calculations also show that to maintain an open end of the SWNT it is necessary that the SWNT adhesion strength to the metal particle is comparable to the cap formation energy of the SWNT end. This implies that the difference between continued and discontinued SWNT growth to a large extent depends on the carbon–metal binding strength, which we demonstrate by molecular dynamics (MD) simulations. The results highlight that first principles computations are vital for the understanding of the binding strength's role in the SWNT growth mechanism and are needed to get accurate force field parameters for MD.

Single-walled carbon nanotubes (SWNTs) have unique properties that make them potential candidates for many technological applications,[1] but many of these applications require cheap and controlled SWNT production. Although research over the past one and a half decades has greatly improved SWNT production leading to orders of magnitude increases in nanotube length and yield,[2−5] there is still relatively poor control of growth with regard to diameter, chirality, and length. Computational modeling of this process has an important role in deepening the understanding of the SWNT growth mechanism at the atomic level,[6−15] together with in situ transmission electron spectroscopy observations.[16−23]

The ultimate challenge of a growth model is the identification of methods for chirality selective production, much like the vision of Richard Smalley of a production unit with two buttons, one to choose the index n and the other to choose the index m, and in such a way fabricate a specific (n,m) SWNT.[24]

The vapor−liquid−solid (VLS) model serves as a phenomenological mechanism for the catalytic growth of nanofibers and nanotubes and is used as a basis for our discussion of SWNT growth.[25−28] The catalyst metal particles serve many purposes such as feedstock decomposition, facilitating the nucleation of nanotubes, healing defects during nanotube growth, and possibly dissolving carbon species. We argue here, however, that an additional critical role is to maintain open ends of growing SWNTs, because previous studies[7,29] and our molecular dynamic (MD) simulations based on a PM3 semiempirical potential energy surface show that in the absence of catalyst particles addition of carbon species or thermal annealing of open SWNT ends leads to their closure. This is due to the instability of the carbon dangling bonds (DBs) at the end of the nanotube. We believe that this is the reason why experimental observations show that SWNTs typically have one free-standing closed end and one open end attached to a catalyst particle.[16,30,31] We focus in this paper on the attractive interactions between the SWNT and the catalyst metal particle and estimate how strong these

* To whom correspondence should be addressed. E-mail: arne.rosen@physics.gu.se.
[†] Göteborg University.
[‡] Uppsala University.
[§] Tyndall National Institute.
[||] University College of Borås.
[⊥] Rice University.
[#] Contributed equally to this work.

10.1021/nl072431m CCC: $40.75
Published on Web 12/28/2007

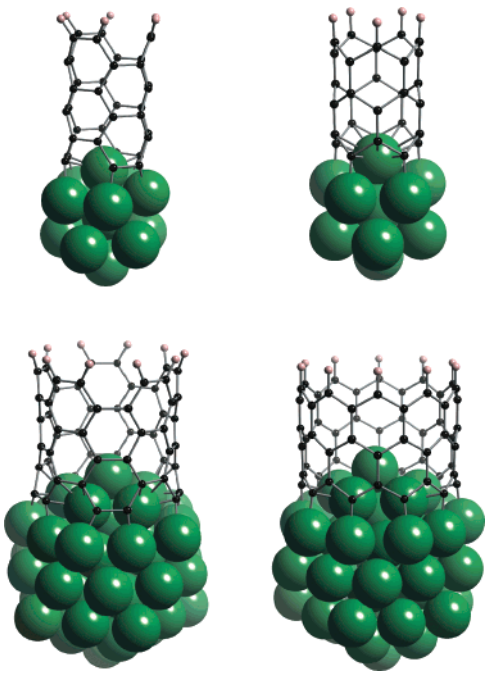

Figure 1. The four model systems used for calculating metal particle−SWNT binding strengths. Top left is a M_{13} icosahedral cluster + (3,3) SWNT fragment; top right is the same M_{13} cluster but with a (5,0) SWNT fragment; bottom left is a bigger M_{55} icosahedral cluster with a (5,5) SWNT; and bottom right is a M_{55} cluster + (10,0) SWNT. The metals M = Fe, Co, Ni, Cu, Pd, and Au were studied.

interactions have to be to overcome competing processes that would terminate growth, such as formation of a cap at the growing end of the SWNT.

We have chosen four different model systems (Figure 1) to be investigated by density functional theory (DFT) calculations: a (5,0) zigzag nanotube adhered to a M_{13} cluster, a (3,3) armchair nanotube adhered to the same M_{13} cluster, a larger (5,5) armchair nanotube adhered to a M_{55} cluster, and finally a (10,0) zigzag nanotube adhered to a M_{55} cluster. The metal, M, is Fe, Co, Ni, Cu, Pd, or Au. Icosahedral structures were chosen for the metal particles, because these are known to be local geometry minima for many metal clusters in this size range. The nanotubes were modeled as three-layered hydrogen-terminated fragments. The M_{13}-(5,0) and M_{13}-(3,3) systems should be considered as test systems, because SWNTs of this size are not usually observed free-standing but inside larger nanotubes or templates.[32,33] The larger M_{55}-(5,5) and M_{55}-(10,0) systems are more realistic, first because metal particles of similar size have been found to grow nanotube-like structures in MD,[11] and second because individual SWNTs of this size are widely found experimentally.[34] Fe, Co, and Ni are selected for these studies because they are the most commonly used catalysts for SWNT growth, and Cu, Pd, and Au are chosen because they are not commonly used as SWNT growth catalysts although they can decompose carbon feedstock.[35−37] In fact, Cu is one of the best catalysts for carbon fiber growth.[37]

The DFT calculations were done using the Vienna ab initio simulation package[38] with the projector augmented-wave method and the Perdew−Wang parametrization of the exchange-correlation energy.[39] The plane-wave basis set energy cutoff was 400 eV, a number that converged the adhesion energies to less than 2 meV/bond. The simulation box for (5,0)-M_{13} was 10 × 10 × 30 Å for M = Fe, Ni, and Co, and 12 × 12 × 30 Å for M = Cu, Au, and Pd. For (5,5)-M_{55} and (10,0)-M_{55}, 15 × 15 × 30 Å and 18 × 18 × 30 Å simulation boxes were used. A Gaussian smearing of 0.05 eV was used for M_{13} systems, while the Methfessel−Paxton scheme[40] was applied to the larger systems that have a more metallic character. The smearing width was adjusted so that the energy associated with the electronic entropy was <0.5 meV/atom. All calculations were spin-polarized and initiated with a total magnetic moment larger than that of the sum of the atomic ground states of the individual cluster and nanotube systems. The total magnetic moments for the SWNT−metal complexes were found to be approximately 20% smaller compared with the bare metal cluster, due to bond creation between the cluster and the carbon nanotube. The structures were relaxed with no symmetry constraints until the total energies were converged to <0.1 meV and average residual forces <0.01 eV/Å. Some of the results were validated with Perdew−Burke−Ernzerhof (PBE) exchange-correlation functional[41] and atom-centered Gaussian basis sets within the program package TURBOMOLE[42] (the details of which will be published elsewhere).

The resulting adhesion energies (divided by the number of DBs for each nanotube) are charted in Figure 2. They span from about 1 to 3 eV/bond with a definite trend: the commonly used catalysts, Fe, Ni, and Co, interact more strongly with the SWNT open end than the less efficient Pd, Cu, and Au catalysts. From this observation, we postulate that sufficiently strong adhesion energy of the SWNT end is a necessary (but not sufficient) condition for SWNT growth.

To understand the critical role of the adhesion strengths and why there might be a limiting value for SWNT growth, we consider the process of the SWNT dissociating from the catalyst particle and forming a capped end. The reaction pictured in Figure 3 can be written as

$$\text{Metal}-\text{SWNT} \rightarrow \text{Metal} + \text{open-ended SWNT} \rightarrow \text{Metal} + \text{capped SWNT} \quad (1)$$

The free energy of this reaction must be positive for growth to be stable under equilibrium conditions; otherwise the nanotube would spontaneously form a cap. The enthalpy change for the first step is the negative value of the adhesion energies (bond strengths in Figure 2 multiplied with the number of DBs). These represent the upper bound of the activation enthalpy for the reaction in eq 1. To quantify the enthalpy change for the full reaction, we constructed capped versions of the (5,5) and (10,0) nanotubes fragments and optimized their geometries. The results are given in Table 1. The strong SWNT−metal bonds for Fe, Co, and Ni give them large positive reaction enthalpies that hinder cap formation, while the metal−SWNT adhesion for Au and Cu particles is not sufficiently strong to maintain the open end of the SWNT. The enthalpy change for

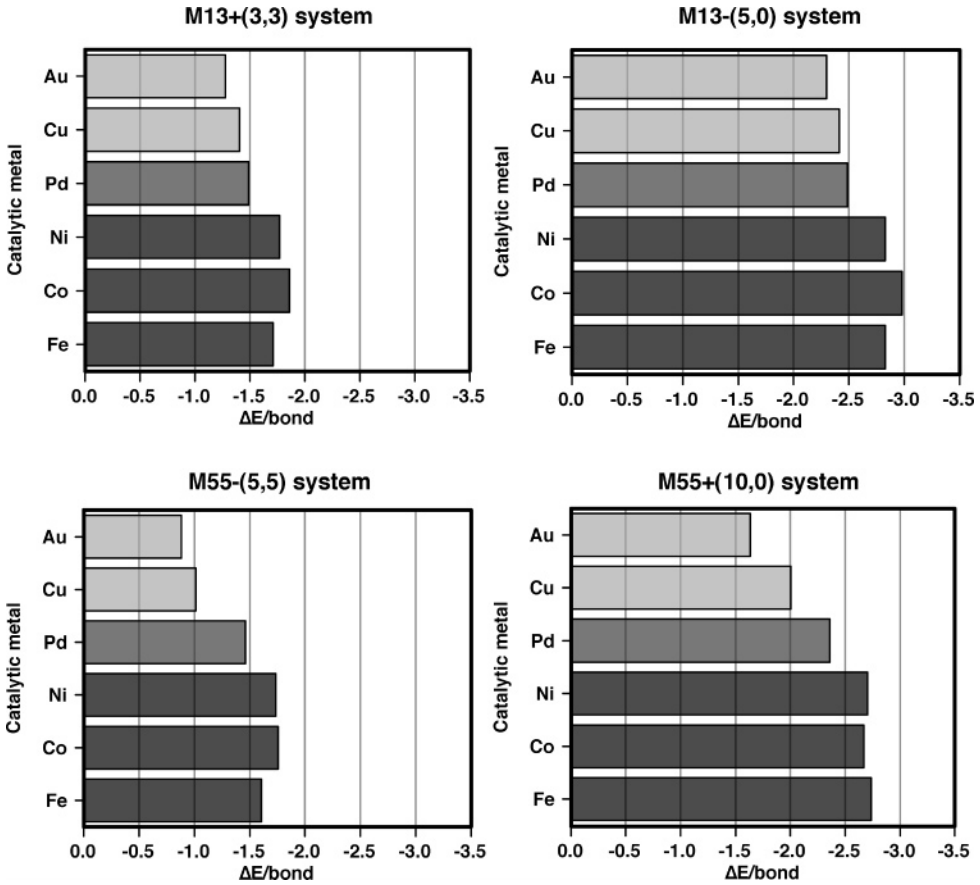

Figure 2. Bond strengths between catalyst particles and open SWNT ends for the four different combinations shown in Figure 1. The catalysts that are commonly used for SWNT growth, Fe, Co and Ni, bind stronger to the SWNT end than Pd, Cu, and Au.

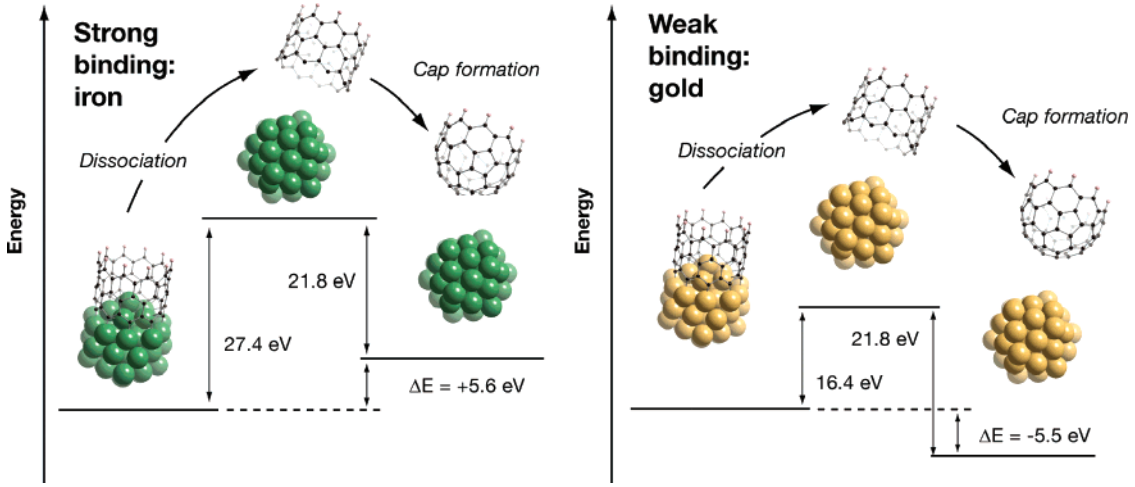

Figure 3. Schematic illustration of the dissociation of a SWNT from a metal catalyst particle. A cap forms in the second step, because the carbon DBs at the nanotube end are no longer stabilized by the catalyst particle. Strong metal−SWNT binding strength (e.g., Fe) prevents spontaneous cap formation ($\Delta E > 0$). But weakly interacting metals like Au do not have sufficient binding strength ($\Delta E < 0$) to prevent cap formation and separation of the SWNT from the catalyst particle.

Pd is only slightly positive, and entropic effects may be important for this metal if the growth temperature is high. Calculating entropy changes is beyond the scope of this paper.

We postulate that a sufficiently strong SWNT−metal adhesion is needed to prevent SWNT closure and hence allow for growth of long nanotubes. A series of MD simulations at 1000 K was performed to study the effect of the nanotube−metal interaction strength in SWNT growth, and a typical example is shown in Figure 4. The simulation method and potential energy surface are the same as in ref 10. Using a carbon metal (C−M) bond strength of 2.5−3.0 eV, which is comparable to the DB formation energy (~2.5 eV), adding one carbon atom to a random surface location of a Fe_{50} catalyst particle every 40 ps, leads to the creation of the SWNT cap as exemplified in Figure 4a. Continuation

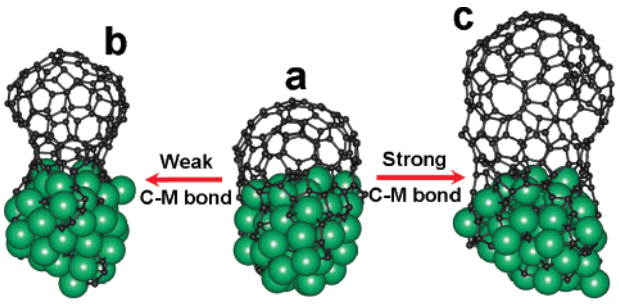

Figure 4. MD simulations of SWNT growth with different carbon−metal interaction strengths. The open end of a carbon cap on a Fe_{50} catalyst particle (a) closes after addition of carbon atoms when the carbon−metal interaction was changed to be weak (a→b) and remains open to support SWNT elongation (a→c) when the carbon−metal interaction is strong, that is, kept the same as for the formation of the initial complex (a).

Table 1. Dissociation Energies for (5,5) and (10,0) SWNTs from M_{55} Catalyst Particles to Capped Nanotube Ends According to Eq 1 (See Figure 3)

metal	dissociation energy (eV) for (5,5) SWNTs	dissociation energy (eV) for (10,0) SWNTs
Fe	2.2	5.6
Co	3.7	4.9
Ni	3.5	5.2
Pd	0.8	1.8
Cu	−3.7	−1.8
Au	−5.0	−5.5

of the MD simulation with unchanged parameters resulted in a longer SWNT with maintained diameter (Figure 4c). But when the C−M bond strength was artificially reduced (1.5−2.0 eV) it resulted in a considerable decrease in the diameter (Figure 4b). In fact, the structure shows resemblance with large fullerene formation. Consequently, our MD simulations show that decreased adhesion strength between the carbon and metal leads to discontinued SWNT growth. The DFT calculations presented here show that the commonly used SWNT catalysts form strong carbon−metal bonds. Thus, the MD trajectories confirm the critical role of strong C−M interactions for the growth of SWNTs.

The importance of the carbon−metal adhesion strength can also be viewed from another perspective: if the adhesion strength is enough to prevent nanotube closure, it may also facilitate expansion of the nanotube end, because increasing the number of carbon−metal bonds would lower the energy of the system. Increasing the SWNT diameter also decreases the curvature energy. However, energy is also required to introduce defects that break the graphene (honeycomb) geometry and that allows for an increase in diameter. Hence, an increase in diameter is thermodynamically favorable if the magnitude of the defect energy is less than the decrease in SWNT−metal adhesion and curvature energies. An extensive study would be required to quantify the defect energies for different nanotubes and defects (as a rough estimate it can be noted that ∼5 eV is required to introduce a heptagon−pentagon pair[43]). However, the bond energies in Table 1 suggest that the SWNT is more likely to expand on Fe, Co, and Ni nanoparticles than on other metals, leading

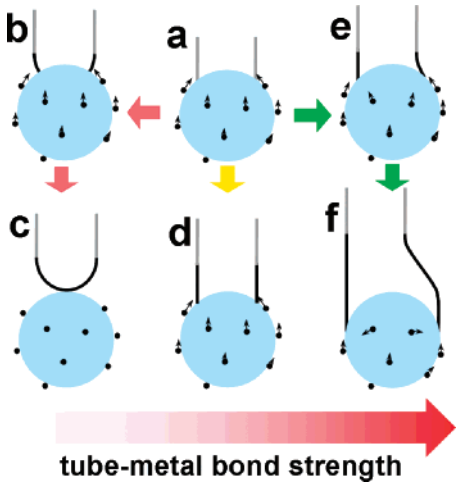

Figure 5. Three possible SWNT growth scenarios from a catalyst particle: I (a→b→c), the nanotube forms a closed cap; II (a→d), the nanotube elongates without a change in diameter; and III (a→e→f), the nanotube elongates and the diameter approaches that of the catalyst particle. The arrow shows the SWNT−catalyst interaction strength giving rise to the three growth scenarios.

to CNT diameters that match the size of the metal particles. This should be possible to confirm experimentally when using seed growth methods to control SWNT diameters,[44] and our results show that the choice of catalyst is crucial for the success of this method.

Figure 5 summarizes three different scenarios that depend on the relative strength of the SWNT−catalyst particle interaction. Scenario I is relevant for particles with weak interaction to the SWNT end and does not promote growth, while scenarios II and III are relevant for SWNT growth. We believe that the binding energy-based scenarios I, II, and III together map out a SWNT growth mechanism that is both intuitive and encompassing. Together with our MD simulations, the DFT results presented in this work indicate that the VLS-based model provides a good basic description for SWNT growth, but that the relative magnitudes of the C−M and DB energies need to be incorporated into the model. Also the directionality of bonds involving carbon, which is much more pronounced than for metal−metal bonds, is important for the formation of carbon nanotubes and dictates the shape of the catalytic nanoparticles. The shape change of apparent crystalline metal particles and if there will be surface or bulk diffusion and the dependence on temperature and the size of the cluster needs to be investigated further and requires a computational study of its own. Some of these issues have been considered for metal surfaces and monoatomic step-edges by Helveg et al., and the mobility of C was shown to be lower than the mobility of Ni adatoms on Ni(111) surfaces.[16,45]

It is important to note that entropic effects may be important at experimental growth temperatures (∼800−1200 K). For example, the catalyst particles change shape during growth, and the curvature of the particle where the SWNT is attached may well affect the adhesion energy. We note that the influence of curvature seems to be small, because the trend and magnitude of carbon−SWNT bonding energies are the same for M_{13} and M_{55} systems studied here, even

though the curvature of the metal clusters is different. In fact, it has been shown that the correct trends in SWNT−metal-binding energy can be simulated using constrained metal rings instead of metals clusters.[46] Further, the presence of nonmetal species on the surface of the catalyst, such as carbon, oxygen, and hydrogen, may also effect the nanotube−catalyst interaction and enable growth from metal catalysts that would not by themselves have sufficiently strong interaction.[47−49] The underlying arguments regarding the importance of strong catalyst adhesions to support SWNT growth and the ability to tune this adhesion to control the nanotube production remain valid, however, whatever the catalyst composition may be. We believe that a growth mechanism based on binding energies/adhesion energies should be used as a basis for the explanations of many CNT-related observations, such as MWNT formation, possibly related to strong/favorable C−M bonds, promotion of catalysts by alloying carbide forming metals (Mo, W, etc.), possibly making metal particle−nanotube adhesion stronger, and effects of heteroatoms (H, O, N, etc.) in the carbon feedstock.

In summary, strong adhesion between SWNTs and the metal clusters from which they are produced is a requirement for SWNT growth. This adhesion must be larger than the energy gained by the SWNT when carbon dangling bonds form a cap. From our first principles computations, this requirement is fulfilled by Fe, Ni, and Co. Cu, Pd, and Au have weaker adhesion strengths but might support growth by virtue of the penalty energy needed to introduce defects into the SWNT honeycomb structure. We deduce that of the many functions of the catalytic metal particles the most important are assisting carbon feedstock cracking, facilitating the nucleation of nanotubes, and stabilizing the open end of the nanotube during growth. We have shown the last of these is required for SWNT growth. Because both the cap formation energy and SWNT−catalyst adhesion energy depend on the chirality of the SWNT, the present model can potentially be used to design possible routes of chirality-controlled growth by careful selection of metals for the catalyst particle. Furthermore, alloying metals by mixing large SWNT adhesion strength metals with varying mole fractions of metals with weak SWNT adhesion strengths could allow one to influence the chirality distributions of the SWNT product. For example, there may be a metal or alloy that gives a positive dissociation energy (see Table 1) for zigzag SWNTs and a negative dissociation energy for armchair SWNTs. Hence, if we can find this metal/alloy we would grow predominantly zigzag SWNTs.

Acknowledgment. The authors are grateful for time allocated on Swedish National Supercomputing facilities and for financial support from the Swedish Research Council, the Swedish Foundation for Strategic Research and Science Foundation Ireland, and the Marie Curie early stage research training (EST) - NANOCAGE.

References

(1) *Carbon Nanotubes: Synthesis, Structure Properties and Applications*; Dresselhaus, M. S., Dresselhaus, G., Avouris, Ph., Eds.; Springer-Verlag: Berlin, 2001. Berlin, 2001.
(2) Iijima, S. *Nature* **1991**, *354*, 56−58.
(3) Ebbesen, T. W.; Ajayan, P. M. *Nature* **1992**, *358*, 220−222.
(4) Zheng, L. X.; O'Connell, M. J.; Doorn, S. K.; Liao, X. Z.; Zhao, Y. H.; Akhadov, E. A.; Hoffbauer, M. A.; Roop, B. J.; Jia, Q. X.; Dye, R. C.; Peterson, D. E.; Huang, S. M.; Liu, J.; Zhu, Y. T. *Nat. Mater.* **2004**, *3*, 673−676.
(5) Hata, K.; Futaba, D. N.; Mizuno, K.; Namai, T.; Yumura, M.; Iijima, S. *Science* **2004**, *306*, 1362−1364.
(6) Lee, Y. H.; Kim, S. G.; Tomanek, D. *Phys. Rev. Lett.* **1997**, *78*, 2393−2396.
(7) Charlier, J.-C.; Vita, A. D.; Blase, X.; Car, R. *Science* **1997**, *275*, 646−649.
(8) Gavillet, J.; Loiseau, A.; Journet, C.; Willaime, F.; Ducatselle, F.; Charlier, J.-C. *Phys. Rev. Lett.* **2001**, *87*, 275504.
(9) Fan, X.; Buczko, R.; Puretzky, A. A.; Geohegan, D. B.; Howe, J. Y.; Pantelides, S. T.; Pennycook, S. J. *Phys. Rev. Lett.* **2003**, *90*, 145501.
(10) Ding, F.; Bolton, K.; Rosén, A. *J. Phys. Chem. B* **2004**, *108*, 17369−17377.
(11) Ding, F.; Rosén, A.; Bolton, K. *J. Chem. Phys.* **2004**, *121*, 2775−2779.
(12) Ding, F.; Rosén, A.; Bolton, K. *Carbon* **2005**, *43*, 2215−2217.
(13) Ding, F.; Bolton, K. *Nanotechnology* **2006**, *17*, 543−548.
(14) Raty, J.-Y.; Gygi, F.; Galli, G. *Phys. Rev. Lett.* **2005**, *95*, 096103.
(15) Li, L.; Reich, S.; Robertson, J. *J. Nanosci. Nanotechnol.* **2006**, *6*, 1290−1297.
(16) Helveg, S.; López-Cartes, C.; Sehested, J.; Hansen, P. L.; Clausen, B. S.; Rostrup-Nielsen, J. R.; Abild-Pedersen, F.; Nørskov, J. K. *Nature* **2004**, *427*, 426−429.
(17) Sharma, R.; Iqbal, Z. *App. Phys. Lett.* **2004**, *84*, 990−992.
(18) Sharma, R.; Rez, P.; Treacy, M. M. J.; Stuart, S. J. *J. Electron Microsc.* **2005**, *54*, 231−237.
(19) Lin, M.; Tan, J. P. Y.; Boothroyd, C.; Loh, K. P.; Tok, E. S.; Foo, Y. L. *Nano Lett.* **2007**, *7*, 2234−2238.
(20) Lin, M.; Tan, J. P. Y.; Boothroyd, C.; Loh, K. P.; Tok, E. S.; Foo, Y. L. *Nano Lett.* **2006**, *6*, 449−452.
(21) Hofmann, S.; Sharma, R.; Ducati, C.; Du, G.; Mattevi, C.; Cepek, C.; Cantoro, M.; Pisana, S.; Parvez, A.; Cervantes-Sodi, F.; Ferrari, A. C.; Dunin-Borkowski, R.; Lizzit, S.; Petaccia, L.; Goldoni, A.; Robertson, J. *Nano Lett.* **2007**, *7*, 602−608.
(22) Sharma, R.; Rez, P.; Brown, M.; Du, G. H.; Treacy, M. M. J. *Nanotechnology* **2007**, *18*, 125602.
(23) Klinke, C.; Kern, K. *Nanotechnology* **2007**, *18*, 215601.
(24) Smalley, R. E. Private communication to Arne Rosén, 2003.
(25) Wagner, R. S.; Ellis, W. C. *App. Phys. Lett.* **1964**, *4*, 89−90.
(26) Baker, R. T. K.; Barber, M. A.; Harris, P. S.; Feates, F. S.; Waite, R. J. *J. Catal.* **1972**, *26*, 51−62.
(27) Saito, Y. *Carbon* **1995**, *33*, 979−988.
(28) Rodríguez-Manzo, J. A.; Terrones, M.; Terrones, H.; Kroto, H. W.; Sun, L.; Banhart, F. *Nat. Nanotechnol.* **2006**, *2*, 307−311.
(29) Kwon, Y.-K.; Lee, Y. H.; Kim, S.-G.; Jund, P.; Tománek, D.; Smalley, R. E. *Phys. Rev. Lett.* **1997**, *79*, 2065−2068.
(30) Li, Y.; Kim, W.; Zhang, Y.; Rolandi, M.; Wang, D.; Dai., H. *J. Phys. Chem. B* **2001**, *105*, 11424−11431.
(31) Zhu, H. W.; Suenaga, K.; Mizuno, K.; Hashimoto, A.; Urita, K.; Hata, K.; Iijima, S. *Small* **2005**, *1*, 1180−1183.
(32) Qin, L.; Zhao, X.; Hirahara, K.; Miyamota, Y.; Ando, Y.; Iijima, S. *Nature* **2000**, *408*, 50.
(33) Wang, N.; Tang, Z. K.; Li, G. D.; Chen, J. S. *Nature* **2000**, *408*, 50−51.
(34) Chen, Y.; Ciuparu, D.; Yang, Y.; Lim, S.; Wang, C.; Haller, G. L.; Pfefferle, L. D. *Nanotechnology* **2005**, *16*, S476−S483.
(35) Bond, G. C.; Thompson, D. T. *Catal. Rev.—Sci. Eng.* **1999**, *41*, 319−388.
(36) Matsumura, Y.; Okumura, M.; Usami, Y.; Kagawa, K.; Yamashita, H.; Anpo, M.; Haruta, M. *Catal. Lett.* **1997**, *44*, 189−191.
(37) Baker, R. T. K. *Carbon* **1989**, *27*, 315−323.
(38) Kresse, G.; Hafner, J. *Phys. Rev. B* **1996**, *54*, 11169−11186.
(39) Perdew, J. P.; Chevary, J. A.; Vosko, S. H.; Jackson, K. A.; Pederson, M. R.; Singh, D. J.; Fiolhais, C.; *Phys. Rev. B* **1992**, *46*, 6671−6687.
(40) Methfessel, M.; Paxton, A. T. *Phys. Rev. B* **1989**, *40*, 3616−3621.
(41) Perdew, J. P.; Burke, K.; Ernzerhof, M. *Phys. Rev. Lett.* **1996**, *77*, 3865−3868.
(42) Ahlrichs, R.; Bär, M.; Häser, H.; Horn, H.; Kölmel, C. *Chem. Phys. Lett.* **1989**, *162*, 165−169.

(43) Meunier, V.; Henrard, L.; Lambin, P. *Phys. Rev. B* **1998**, *57*, 2586−2591.
(44) Wang, Y.; Kim, M. J.; Shan, H.; Kittrell, C.; Fan, H.; Ericson, L. M.; Hwang, W. F.; Arepalli, S.; Hauge, R. H.; Smalley, R. E. *Nano Lett.* **2005**, *5*, 997−1002.
(45) Abild-Pedersen, F.; Nørskov, J. K.; Rostrup-Nielsen, J. R.; Sehested, J.; Helveg, S. *Phys. Rev. B* **2006**, *73*, 115419.
(46) Larsson, P.; Larsson, J. A.; Ahuja, R.; Ding, F.; Yakobson, B. I.; Duan, H. M.; Rosen, A.; Bolton, K. *Phys. Rev. B* **2007**, *75*, 115419.
(47) Zhou, W.; Han, Z.; Wang, J.; Zhang, Y.; Jin, Z.; Sun, X.; Zhang, Y.; Yan, C.; Li, Y. *Nano Lett.* **2006**, *6*, 2987−2990.
(48) Takagi, D.; Homma, Y.; Hibino, H.; Suzuki, S.; Kobayashi, Y. *Nano Lett.* **2006**, *6*, 2642−2645.
(49) Bhaviripudi, S.; Mile, E.; Steiner, S. A., III; Zare, A. T.; Dresselhaus, M. S.; Belcher, A. M.; Kong, J. *J. Am. Chem. Soc.* **2007**, *129*, 1516−1517.

NL072431M